A Computational Pipeline for Design and Fabrication of Building Slab Units with 3D Printing and Robotic Production Cells

Yuchen Tang[1]**, Emad Shakour**[1]**, Oded Amir**[1] **and Rafael Sacks**[1]

[1]Faculty of Civil and Environmental Engineering, Technion – Israel Institute of Technology, Israel

yuchen.tang@campus.technion.ac.il, semad@technion.ac.il, odedamir@technion.ac.il, cvsacks@technion.ac.il

Abstract -

Full-scale 3D concrete printing for horizontal structural components is challenging due to large unsupported spans, early-age material instability, and geometric limitations of extrusion-based processes. A practical solution is to fabricate modular slab units by printing only the structural ribs of the slab while casting the top and bottom layers conventionally and achieving composite action through post-tensioning. This paper presents a computational pipeline for the integrated design and feasibility evaluation of such hybrid slab units. A design pipeline generates topology-optimized rib layouts, segments the slab into prefabricated units, refines local structural features, and performs constructability checks before producing a detailed BIM model. A complementary simulation pipeline evaluates fabrication and feasibility of erection within the same workflow. Motion-level simulations in Gazebo assess reachability, collision avoidance, and lifting trajectories for production cells, while rule-based risk evaluators identify constraints beyond rigid-body simulation.

Keywords -

3D concrete printing; Constructability evaluation; Hybrid construction; Ribbed slab units; Topology optimization; Robotic simulation.

1 Introduction

Recent advances in 3D concrete printing have enabled efficient automated fabrication of vertical components, such as walls and columns, where material is deposited layer by layer in a predominantly vertical direction and is continuously supported[12, 19]. In contrast, full-scale slab printing remains largely infeasible. Slabs require depositing fresh material horizontally over large spans, which requires traditional formwork and cannot be printed. In addition, many current extrusion-based systems are designed for prismatic, single-direction geometries that are not well suited to multi-directional structural behaviour.

An alternative is to prefabricate units in production cells where printing is restricted to the structural ribs of the slab. In such a hybrid system, ribs can be generated using topology optimization to align with principal stress trajectories. The top and bottom layers can be cast conventionally, and post-tensioning can be used to activate composite action and enable large-span performance. The slab can be segmented into prefabricated units to satisfy transportation and lifting constraints. However, this hybrid approach produces a highly coupled workflow involving rib printing, concrete casting, unit lifting, on-site assembly, and post-tensioning. Assessing feasibility across this workflow is challenging due to geometric, structural, and robotic limitations.

In this work, we formulate a computational pipeline for the integrated design and feasibility evaluation of such slab units. The pipeline is structured into two tightly coupled components:

1. **Design**: design of hybrid ribbed slab units, from initial input conditions to parametric BIM geometry, with a focus on topology optimization. This workflow not only serves to provide input for simulation of the system as a whole, it also forms the basis for a fully parametric and automated design system for eventual production of such slab units.
2. **Simulation**: simulation of the fabrication process that integrates robot motion and 3D printing equipment with rule-based scheduling and risk evaluation, and simulation of the erection and post-tensioning process on site.

The paper provides a background review of the state-of-the art for fabrication of horizontal elements with 3D printing in building construction, software for structural design and topology optimization, software for simulation of robotic and 3D printing production cells, and software for 4D planning and analysis of construction operations. It then details feasible computational workflows for each of the two steps listed above.

2 Related work

2.1 3D printing of structural components

3D printing of cementitious materials, particularly 3D concrete printing (3DCP), is gaining interest for enabling complex geometries and material-efficient structural design. This is increasingly relevant given the difficulty of realizing optimized concrete structures using conventional formwork-based construction.

3DCP allows formwork-free fabrication of complex geometries, but applications have primarily focused on vertical elements. Horizontal members remain challenging due to bending-dominated response and limited reinforcement options, which motivates compression-dominated designs. For beams and slabs, prestressing enables such behavior and improves structural performance [11], while also supporting segmental post-tensioned and modular construction.

Hybrid construction, combining printed stay-in-place formwork with cast concrete, has emerged as an alternative approach. Initially applied to vertical elements, it has recently been extended to horizontal members [9]. These developments highlight the potential of 3DCP and the need for integrated computational workflows that link structural design, optimization, fabrication, and construction.

2.2 Structural optimization

Structural optimization, particularly topology optimization, enables substantial material savings by aligning geometry with internal force flow. Owing to its design freedom, topology optimization can be tailored to address multiple design stages, from conceptual layout to fabrication-aware realization.

A simultaneous shape and topology optimization framework for prestressed concrete systems was introduced in [1, 2] and later integrated with 3DCP through CAD-based interpretation and post-tensioned fabrication [16]. This demonstrated its potential for segmented, prestressed printed structures, while also highlighting the need for tighter design–fabrication integration. The framework has since been extended to fully three-dimensional free-form optimization of prestressed beams and slabs [14], which is adopted in the present study.

An additional key challenge in realizing optimized geometries with 3DCP is early-age material behavior during printing. To address this, optimization formulations incorporating buildability constraints have been proposed to ensure printability [7, 13].

Overall, these developments demonstrate the potential of structural optimization for efficient 3DCP, particularly when structural, material, and fabrication considerations are integrated within a unified design framework.

2.3 Robotics simulation in construction

Robotics simulation environments such as Gazebo and V-REP have been increasingly used in construction research to visualize and validate robotic workflows [5]. However, most studies treat simulation as a visualization or debugging tool, focusing on kinematics and collision avoidance, rather than using it as part of a risk-evaluated construction logic. The proposed methodology embeds motion-level simulation into a validation pipeline, combining Gazebo-based action simulation with external rule-based evaluators to assess constructability, printability, and erection risks of full slab systems—bridging the gap between motion simulation and feasibility-driven design.

2.4 4D CAD simulation for construction

4D CAD is a well-established method for evaluating construction methods and processes [10]. It is commonly used for complex construction projects and numerous software tools offer 4D functionality. However, they are restricted to predetermined motion paths and fixed element geometries - they lack the operational detail and the physics engines needed for planning and validating the motion of robotic and 3D concrete printing machinery needed for design of automated production cells contemplated in this work. For this reason, we use Gazebo Simulation[8] with Robotic Operating System (ROS) integration to plan and validate the constructability of slab units.

2.5 Software interoperability

The increasing use of BIM, parametric modeling, and robotics in construction demands robust software interoperability. However, workflows often remain fragmented, with tools such as Revit, Rhino/Grasshopper, FEM solvers, and ROS/Gazebo used in isolation. Prior efforts have explored parametric and BIM-integrated workflows, but few address interoperability from early design to robotic fabrication [6, 15, 18]. The proposed pipeline demonstrates a connected chain: BIM authoring → parametric modeling → structural analysis → robotic simulation, with data exchanged through mesh conversion, scripting, and task encoding—supporting a full feedback loop across design and construction domains.

3 Solution overview

The proposed method integrates design and simulation into a two-stage computational pipeline.

First, a Design Pipeline processes an input architectural slab layout into a manufacturable set of hybrid precast units. This design stage encompasses geometry extraction, global topology optimization, segmentation into units, local structural design, constructability checks, and parametric BIM geometry generation.

Second, a Simulation Pipeline takes the BIM model as input and evaluates feasibility and safety. It converts geometry into formats suitable for robotic simulation, defines tasks, generates toolpaths and trajectories, sets up Gazebo scenes, runs simulations for both fabrication and erection, and complements Gazebo with rule-based risk evaluators.

The two pipelines are linearly connected by default: the output of the Design Pipeline feeds into the Simulation Pipeline sequentially. Critically, the framework also supports an iterative feedback loop (stage S7) whereby detected risks in simulation prompt design modifications in earlier stages, enabling design-for-constructability through repeated cycles if needed. This ensures that the slab system not only meets structural and architectural requirements but can also be fabricated with robotic 3D-printing and assembled on-site.

4 Design pipeline

4.1 D1 – Input and boundary conditions

The Design pipeline (Figure 1) begins with a formal definition of the slab design problem, consolidating all relevant architectural, structural, and constructability parameters. In this stage, the system gathers and encodes the boundary conditions, design objectives, and fabrication constraints that govern the remainder of the pipeline.

Architectural input includes the slab layout, openings, and support configuration, typically extracted from BIM models in Revit or IFC format. Structural input includes material properties , design load cases, and permissible deflection criteria. Constructability-related constraints are also explicitly defined. These include limits on maximum unit weight based on crane capacity, unit dimensions based on transportation and printer workspace, and minimum rib thickness or curvature radius based on extrusion nozzle geometry.

All inputs are consolidated into a structured configuration file, which may be implemented as a .json or .yaml file and is readable by downstream modules. Each parameter is associated with its source and its status. This configuration serves as the canonical reference for the remainder of the pipeline, guiding geometry extraction, optimization, segmentation, constructability checks, and simulation. This stage enhances clarity, reusability, and cross-project consistency.

4.2 D2 – Geometry extraction and pre-processing

This stage converts architectural slab definitions from BIM into a clean and analysis-ready geometric domain. The process begins by extracting the slab's physical outline and internal voids using Dynamo for Revit or Python scripts with IfcOpenShell for IFC-based models. Structural supports—such as columns, load-bearing walls, or beams—are identified by intersecting BIM elements with the slab geometry. These intersections are translated into support boundary conditions for structural analysis. Unlike conventional approaches that assume regular or rectangular shapes, this method accepts arbitrary slab boundaries, including non-convex, curved, and multiple-voided geometries.

The extracted geometry is then pre-processed to remove inconsistencies and modeling noise. Small fillets, disconnected edges, and planar irregularities are cleaned. The cleaned geometry is exported as a three-dimensional solid mesh and used as input for 3D topology optimization in stage D3.

4.3 D3 – Global topology optimization

This stage applies three-dimensional topology optimization to generate the global rib-and-void geometry of the slab. Using the meshed slab domain from Stage D2 and the material and boundary conditions from Stage D1, the slab is modeled as a three-dimensional solid domain. The optimization follows the prestressed concrete topology optimization framework developed in [14], incorporating common prestressed concrete design practices in the objective formulation and volume constraint, including the structural effects of post-tensioning on load transfer and stiffness. We note that the framework incorporates simultaneous optimization of the concrete distribution and of the tendons' geometry, such that the effect of prestressing is captured from the early design stage by means of equivalent forces.

An illustrative example is presented for a simply supported prestressed concrete slab with dimensions $12.0 \times 12.0 \times 0.36$ m, subjected to uniformly distributed dead and live loads of 10 kN/m^2 each. The top and bottom two element layers are prescribed as solid material, corresponding to a thickness of 0.06 m for the top and bottom slab parts, while the optimization is restricted to the intermediate region to identify an efficient rib layout connecting the lower and upper concrete layers. The overall allowable concrete volume fraction, including the top and bottom parts, is limited to 50%. A mid-height cross-section illustrating the top and bottom parts of the optimized design is shown in Figure 2.

The resulting rib geometry is freeform, shaped by the optimized layout of post-tensioning cables and additional rib stiffeners. The output is a three-dimensional solid geometry capturing the full layout of ribs and internal voids, which is exported as an STL mesh or converted into editable BREP surfaces representing the printable and structurally informed volume of the slab core.

4.4 D4 – Unitization (segmentation into prefabricated units)

After the generation of the global rib geometry, the slab must be divided into constructible units suitable for robotic fabrication, transport, and on-site lifting. This unitization

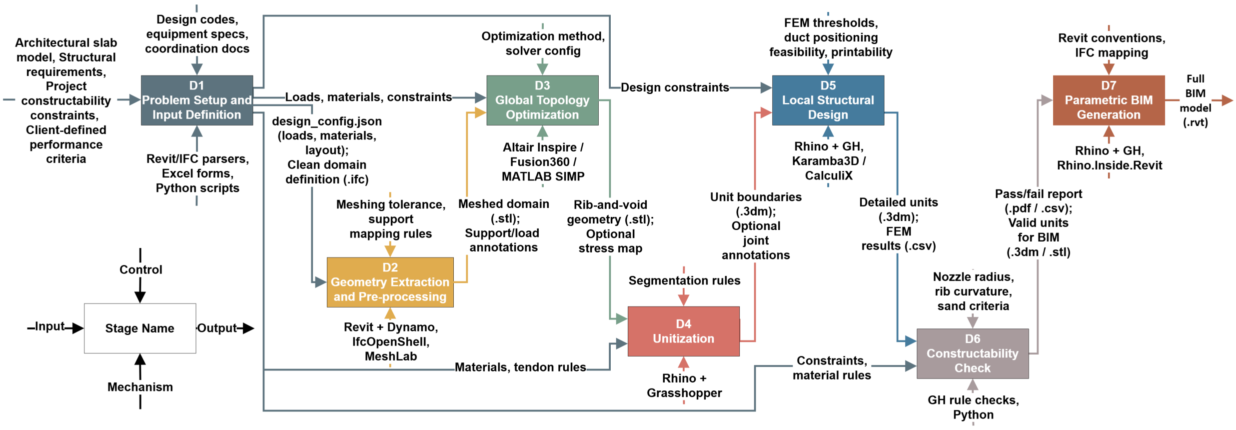

Figure 1. Design pipeline using IDEF0 notation

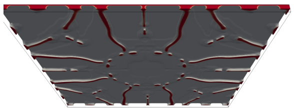

(a) Top layer.

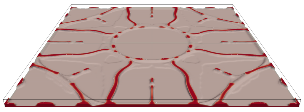

(b) Bottom layer.

Figure 2. Optimized slab geometry.

stage defines the boundaries between slab modules and directly affects their structural continuity, printing feasibility, and assembly workflow. This modular decomposition aligns with DFMA-oriented prefabrication approaches [4].

Segmentation begins by identifying regions of the rib network where natural breaks can occur. Cutting lines are guided by the rib topology: they are deliberately routed through void zones or rib junctions, and avoid slicing directly through the middle of major load-bearing ribs. The goal is to minimize the disruption of continuous load paths and reduce the total rib cross-sectional area that must be interrupted. Curved or angled segmentation lines are allowed if they better follow the rib architecture, rather than imposing an artificial rectilinear grid.

Each proposed unit is then evaluated against fabrication and logistics constraints defined earlier in stage D1. These include limits on unit footprint, estimated weight for lifting, and clearance requirements for handling equipment. At this stage, the evaluation is rule-based and geometric—no finite element analysis is performed. Units that violate basic constraints are iteratively re-partitioned. Where unavoidable, segmentation boundaries that intersect rib regions are marked for later reinforcement or anchorage detailing in stage D5.

The unitization workflow is implemented in Rhino using Grasshopper, with rib geometry imported as STL or mesh files from D3. Segmentation curves are generated and refined parametrically, then exported as BREP sub-volumes. These definitions are passed to downstream detailing (D5) and BIM integration (D7), ensuring traceability and continuity across design stages.

4.5 D5 – Local structural design and detailing

Once the slab has been divided into prefabricated units, each segment undergoes local structural design to ensure printability, post-tensioning feasibility, lifting safety, and full structural performance. This stage converts the global optimization mesh into detailed, buildable geometry.

Since the ribs generated in stage D3 are non-parametric and typically represented as STL meshes, a geometric reconstruction process is performed. The discrete optimization mesh is converted into parametric BREP geometry through cross-section sampling and lofting to enable downstream detailing.

Tendon ducts are embedded within the rib volume using solid Boolean operations. Each duct follows a defined path from one anchorage point to another, and is constrained by minimum curvature, wall clearance, and interface geometry. At rib intersections, ducts are either limited to principal structural directions or offset vertically to avoid conflict. This ensures smooth threading and successful anchorage during post-tensioning. Void regions between ribs form unoccupied spaces that are temporarily filled with sand to support the top concrete layer during casting. Rib spacing and topology are adjusted to avoid excessive overhangs and ensure that voids remain accessible for sand placement and removal.

The slab unit is completed with a bottom and top concrete layer, each containing its own steel mesh reinforcement. The three components form a sandwich structure. For enhanced interlayer shear resistance, starter bars may be embedded into or alongside the ribs. In high-curvature or support-bearing regions, ribs may be thickened, or vertical reinforcement zones introduced. Each unit undergoes structural validation using lightweight finite element models, such as Karamba3D or CalculiX, to evaluate lifting deformation, internal stress distribution, and tendon alignment, reflecting the influence of prestressing on structural response. Units that fail to meet structural or fabrication constraints are flagged for revision of rib geometry, duct routing, or anchorage region shaping.

The output of stage D5 is a fully detailed, fabrication-ready slab unit model—including solid ribs, tendon ducts, sand-supportable voids, and cast concrete layers—passed to stages D6 for constructability verification and D7 for BIM integration.

4.6 D6 – Constructability check

Before the slab unit models proceed to simulation and BIM integration, each unit undergoes a constructability check to ensure that the geometry complies with fabrication, transportation, and assembly constraints, verifying whether the geometry can be realistically fabricated, lifted, and handled. This stage checks a series of rule-based geometric and physical constraints, such as: minimum rib thickness and printable curvature radius to avoid nozzle failure or material sagging; maximum unit dimensions and weight based on gantry size, crane capacity, and transport limits; duct minimum bending radius to ensure tendon threading is possible.

These checks are implemented in Grasshopper using parametric scripts. Thresholds and constraints are imported from stage D1 and updated as needed. Units that fail any criteria are flagged for revision in rib geometry, segmentation boundary, or detailing logic.

The constructability check also produces embedded metadata such as center of gravity, expected lifting points, and estimated assembly tolerances. This information is essential for planning site erection (S5) and exporting to BIM (D7).

The output of stage D6 is a verified set of slab units with constructible geometry and constraint-satisfying properties. These models are then passed to the simulation pipeline.

4.7 D7 – Parametric BIM generation

After structural and constructability validation, each slab unit is converted into a parametric BIM representation for coordination, documentation, and integration with broader project workflows. This ensures the design outputs from previous stages are compatible with industry-standard BIM platforms and ready for simulation, fabrication, and site operations.

Each slab unit is composed of multiple components—including cast-in-place top and bottom concrete layers, 3D-printed rib structures, embedded tendon ducts, temporary voids, and reinforcement meshes. These are modeled in Rhino and Grasshopper, then transferred into Revit using the Rhino.Inside.Revit framework. Geometries are classified into appropriate Revit categories (e.g., floors, structural framing, and generic models) with embedded metadata as Revit instance parameters to support scheduling and clash detection.

The final output of stage D7 is a complete, structured BIM model comprising all prefabricated slab units, their internal components, and associated metadata. It serves as the authoritative digital representation of the system and links design, fabrication, and erection phases into a unified digital workflow.

5 Simulation pipeline

5.1 S1 – Model conversion

The Simulation Pipeline (Figure 3) begins by converting the detailed BIM output from D7 into simulation-ready assets for robotic and construction environment modeling. Each slab unit is exported from BIM (Revit or Rhino3D) as a triangulated mesh in STL or OBJ format. Supporting elements such as columns, walls, and floors are also extracted to define the physical context for virtual erection. Prior to export, a mesh simplification step is applied using tools like MeshLab or open3D to reduce polygon count, improving simulation efficiency without altering the slab's global shape. Geometry export is automated via scripting, while the assignment of lifting points and tendon tags currently requires manual annotation in Grasshopper or Revit. These assets are converted into Gazebo-compatible formats: static objects are encoded in Simulation Description Format (SDF), while movable objects (e.g., slab units subject to lifting) are converted into Unified Robot Description Format (URDF) with optional joint definitions and inertial tags.

Embedded metadata (e.g., element ID, volume, mass) are extracted automatically from the BIM model. Additional metadata, such as tendon duct alignment or grouting zone tags, can also be embedded using Gazebo plugins for later validation. The result is a library of simulation-ready models reflecting the BIM geometry, but optimized for robot control and physical simulation in Gazebo. This library is used in later stages (S4–S6) for kinematics, task execution, and collision-based validation.

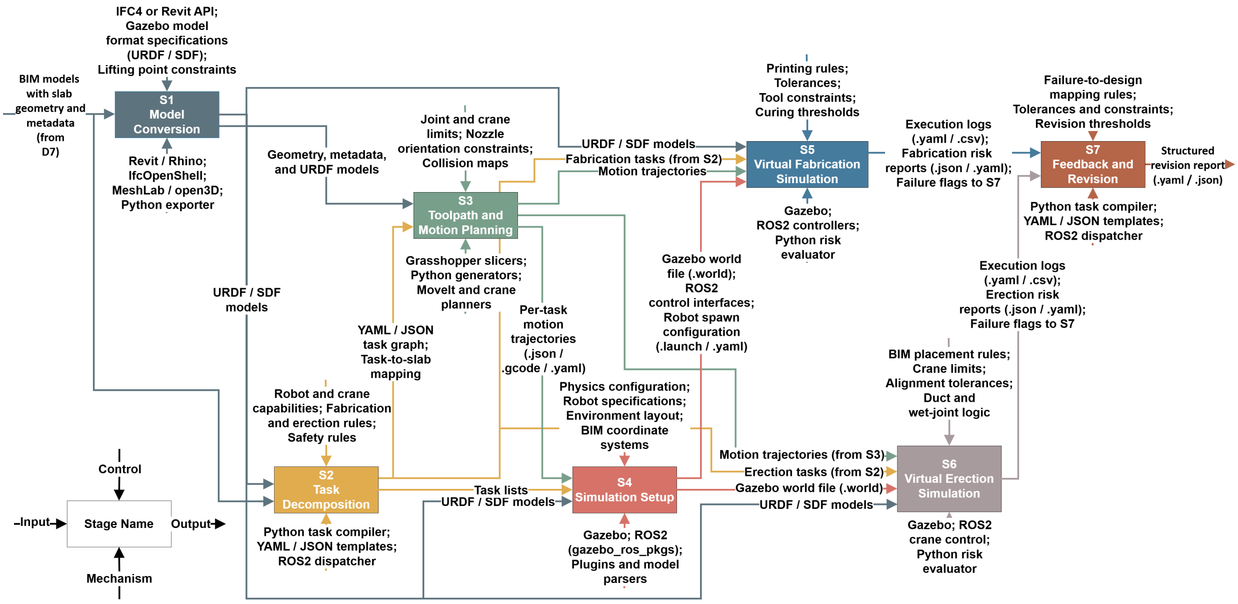

Figure 3. Simulation pipeline using IDEF0 notation

5.2 S2 – Task decomposition and sequencing

This stage defines a structured execution plan for fabrication and erection, decomposing the overall slab construction process into discrete, simulation-ready tasks. Based on the BIM-derived models and metadata from S1, each slab unit is associated with a specific sequence of robotic or crane-based operations. There are eight fabrication steps, three storage and transportation steps, and six erection steps. Most geometry-to-task mappings—such as identifying target slab units and assigning agents based on lifting points or print zones—are automatically inferred from BIM metadata or spatial relationships, while certain parameters (e.g., pour speed or human involvement) still require manual annotation at this stage.

Each task is encoded in a machine-readable YAML or JSON format that specifies: 1) Task type (e.g., print_ribs, place_ducts) 2) Target slab unit or geometry 3) Assigned agent (gantry, robotic arm, crane) 4) Required inputs (e.g., toolpath file, lifting anchor) 5) Temporal dependencies (e.g., curing complete before lifting).

This results in a Directed Acyclic Graph (DAG) of tasks that enables logical sequencing and parallelization. The task graph can be parsed and executed by ROS2 nodes, providing a control interface between planning and simulation. Task definitions can also be linked to BIM elements for 4D scheduling or progress monitoring. Where available, task hints embedded in BIM models—such as lifting zones or build order tags—are incorporated. The generated graph serves as the input for motion planning (S3) and simulation execution (S5–S6).

5.3 S3 – Toolpath and motion planning

This stage translates each task from the construction graph (S2) into executable robot motion. For fabrication, geometric inputs from S1 are automatically sliced into layer-based toolpaths, exported as .json or .gcode files. Each path includes 3D positions, print speed, nozzle orientation, and pause points. Ducts are inserted using a “pause-and-insert-from-above” method. After printing several layers of the rib, ducts are lowered vertically into grooves and sealed by continuing the print (conceptually consistent with in-process insertion and pause-and-insert strategies reported in [17, 3]). This method avoids lateral interference and fits well with robot-assisted insertion.

For each path, ROS2 MoveIt performs inverse kinematics and collision checks. Gantries and arms are automatically evaluated for reachability, joint limits, and obstacle avoidance. Unreachable or unsafe segments are flagged for revision. Tasks like sand filling and mesh placement are handled as partially scripted, parametric sweeps or pick-and-place motions, with manual definition of start/end poses.

Erection planning uses simplified crane kinematics. Given start/end poses from S2, safe lifting paths are automatically generated considering swing limits and clearance from obstacles. The planner ensures loads stay within the crane’s envelope and avoids sharp accelerations.

All results are saved in ROS2-compatible formats (.json, .yaml), indexed by unit ID and task name. These trajectories are passed to the simulation system in S5–S6, forming the robotic execution layer.

5.4 S4 – Simulation environment setup in Gazebo

This stage builds a simulation-ready digital twin in Gazebo that replicates both the fabrication and site environments for the slab system. The environment integrates geometric models (from S1), robotic tasks (from S2), and planned motion trajectories (from S3), enabling time-sequenced motion playback, real-time collision checking, and dynamic constructability validation. The simulation environment comprises two zones: 1) a factory layout containing the printing gantry, formwork, and manipulators, and 2) a site layout including BIM-derived structural supports, the crane system, and positioning frames.

Each object is instantiated from its SDF or URDF model with its physics properties. ROS2 control plugins are attached to each robot to enable real-time command execution. For instance, the gantry receives Cartesian print trajectories; the crane interprets lifting paths and winch cable lengths; and all actions are synchronized via ROS2 messages. Slab units spawn with embedded metadata to support accurate tracking and placement.

Environmental dynamics such as gravity, surface contact friction, and optional wind disturbances are enabled. The goal is to achieve realistic behaviour of printed structures, suspended loads, and placement operations. Contact modeling between slab units and supports allows validation of alignment and load transfer.

By the end of S4, a complete virtual environment is assembled, with all elements positioned in BIM-coherent coordinates. This environment forms the runtime context for executing and analyzing fabrication and erection tasks in S5 and S6.

5.5 S5 – Fabrication simulation

This stage executes each prefabrication task in the virtual environment built in S4, validating robotic execution under physical constraints. Using ROS 2 controllers, each robot agent performs the motion trajectories generated in S3. Gazebo simulates kinematics, contact, and collisions based on physical parameters, while task scheduling and execution follow the construction graph from S2.

The fabrication sequence includes: bottom mesh placement, bottom-layer concrete casting, rib printing with duct insertion pauses, sand filling, top mesh placement, and top-layer casting. The rib printing process follows layered paths; at designated heights, the print head pauses and a duct insertion motion is executed.

A custom Risk Evaluator monitors execution in real-time, flagging issues such as nozzle collisions, reachability violations, or curing time constraints based on task timestamps and predefined rule-based thresholds (e.g., minimum clearance distance, reach limits, and time intervals). All fabrication actions are logged with timestamps, unit IDs, task names, and pass/fail tags. Warnings from the Risk Evaluator are saved in structured YAML/JSON reports and linked to slab unit metadata. If a failure is detected the system records which unit and stage requires revision. These reports are forwarded to stage S7 for design iteration.

5.6 S6 – Erection simulation

This stage simulates the robotic and crane-assisted assembly of prefabricated slab units in a virtual construction site, evaluating geometric feasibility, placement accuracy, and interface alignment. Using the digital twin environment established in S4, each slab unit is lifted, positioned, and logically integrated into the structural frame.

A crane model, a URDF with boom joints and winch mechanism, is commanded via ROS2 controllers to follow the lifting trajectories defined in S3. Each unit is lifted from the ground or factory bed, transported across the site, and lowered onto structural supports derived from the BIM geometry. Upon placement, the system verifies whether the unit rests stably on pre-positioned temporary supports. Contact is evaluated using bounding box intersections and pose thresholds (e.g., allowable tilt angle and support coverage ratio). If a corner lacks adequate support or the unit exceeds tilt limits, the Risk Evaluator flags it for temporary shoring.

Adjacent slabs undergo geometric validation for duct alignment and wet joint feasibility. Co-oriented duct outlets within tolerance (e.g., positional and angular deviation limits) enable logical tendon threading, while misalignments trigger a redesign flag. Post-tensioning is abstracted as a logic state rather than a physical simulation, while its structural effects are incorporated in the design stage through topology optimization and structural analysis, set only when valid alignment and closeable joint gaps are confirmed.

All outcomes—placement success, duct alignment, propping needs, and tendon connection feasibility—are logged per slab unit in structured YAML/JSON records. These records are passed to the feedback module (S7), enabling targeted revision in design.

5.7 S7 – Feedback loop and design revision

This stage closes the simulation-design loop by interpreting the results from virtual fabrication (S5) and erection (S6), and routing issues back to the appropriate stages of the design pipeline (D3–D6) for revision. The goal is to enable targeted design refinement without restarting the entire process.

6 Discussion and conclusion

This paper proposed a dual-pipeline method for the design and simulation of 3D-printed slab systems with embedded post-tensioning, integrating a D-stage design pipeline (D1–D7) with a S-stage simulation pipeline (S1–S7). Unlike prior work focusing on small-scale printing or isolated robotic tasks, our pipeline supports full-scale prefabricated units with embedded structural logic, and accounts for site-level erection and post-tensioning.

A key contribution is the integration of rule-based feedback between simulation and design, enabling early-stage decisions to be evaluated against real-world constraints. The structured task graph format and use of ROS2+Gazebo ensure that both fabrication and erection steps can be virtually tested before deployment.

Limitations include the simplification of material behaviors and the lack of full automation in geometry-to-task mapping in the simulation stage . Future work will extend risk evaluation to cover time-dependent rheology and incorporate real-world feedback from physical trials. The proposed pipeline serves as a foundation for digital twin–enabled robotic prefabrication in building-scale applications.

Acknowledgements

This work was funded by the European Union under Grant Agreement No. 101162318 (AM2PM).

References

[1] O. Amir and E. Shakour. Simultaneous shape and topology optimization of prestressed concrete beams. *Structural and Multidisciplinary Optimization*, 57(5):1831–1843, 2018. Publisher: Springer.

[2] O. Amir and E. Shakour. Topology optimization of post-tensioned concrete beams. In *Proceedings of IASS Annual Symposia*, volume 2018, pages 1–8. International Association for Shell and Spatial Structures (IASS), 2018. Issue: 19.

[3] G. Bai, L. Wang, Z. Li, Y. Qu, and G. Ma. Integrating prestress into 3d printed ultra-high performance concrete composite beams for superior flexural performance. *Engineering Structures*, 343:121255, 2025.

[4] D. Dong, Y. Zou, H. Pan, G. Zhou, Y. Feng, and Y. Tang. Dfma-oriented modular and parametric design and secondary splitting of vertical pc components. *Scientific Reports*, 13(1):3457, 2023.

[5] S. M. Kargar, B. Yordanov, C. Harvey, and A. Asadipour. Emerging trends in realistic robotic simulations: A comprehensive systematic literature review. *IEEE Access*, 12:191264–191287, 2024. ISSN 2169-3536.

[6] S. Kim, M. Peavy, P.-C. Huang, and K. Kim. Development of bim-integrated construction robot task planning and simulation system. *Automation in Construction*, 127:103720, July 2021.

[7] M. Mogra. Design optimization of building elements for manufacturing using 3D concrete printing. Master's thesis, Technion - Israel Institute of Technology, 2023.

[8] Open Source Robotics Foundation. Gazebo simulator, 2024. URL `https://gazebosim.org/`.

[9] S. Raza, M. Sakha, Z. Hassan, B. Manshadi, X. Wang, H. Fan, B. Dillenburger, and M. Shahverdi. Flexural behavior of stay-in-place load-bearing 3d-printed concrete formwork for ribbed slabs. *Engineering Structures*, 338:120531, 2025.

[10] R. Sacks, G. Lee, L. Burdi, and M. Bolpagni. *BIM Handbook: A Guide to Building Information Modeling for Owners, Designers, Engineers, Contractors and Facility Managers*. John Wiley and Sons, Hoboken, NJ, 4th edition, 2025. ISBN 978-1-394-22222-3.

[11] T. A. M. Salet, Z. Y. Ahmed, F. P. Bos, and H. L. M. Laagland. Design of a 3D printed concrete bridge by testing. *Virtual and Physical Prototyping*, 13(3): 222–236, 2018.

[12] R. Sedghi, K. Rashidi, and M. Hojati. Large-scale 3d wall printing: From concept to reality. *Automation in Construction*, 159:105255, 2024.

[13] E. Shakour and O. Amir. An integrated computational framework for structural optimization of prestressed concrete structures with 3d-printed formwork. *engrXiv*, 2026.

[14] E. Shakour, A. Shaked, and O. Amir. Topology and shape optimization of 3D prestressed concrete structures. *Engineering Structures*, 321:118936, 2024.

[15] M. Slepicka, S. Vilgertshofer, and A. Borrmann. Fabrication information modeling: Interfacing building information modeling with digital fabrication. *Construction Robotics*, 6(2):87–99, June 2022. ISSN 2509-8780.

[16] G. Vantyghem, W. D. Corte, E. Shakour, and O. Amir. 3D printing of a post-tensioned concrete girder designed by topology optimization. *Automation in Construction*, 112:103084, 2020. ISSN 0926-5805.

[17] Z. Wu, A. M. Memari, and J. P. Duarte. State of the art review of reinforcement strategies and technologies for 3d printing of concrete. *Energies*, 15(1):360, 2022.

[18] S. Zhang, Y. Tang, Y. Zou, H. Yang, Y. Chen, and J. Liang. Optimization of architectural design and construction with integrated bim and plm methodologies. *Scientific Reports*, 14(1):26153, 2024.

[19] Y. Zhi, H. Chai, T. Teng, and M. Akbarzadeh. Automated toolpath design of 3d concrete printing structural components. *Additive Manufacturing*, 100: 104662, 2025.